Published in final edited form as:
Microsc Microanal. 2013 August ; 19(4): 799–807. doi:10.1017/S1431927613000457.

The Conserved Tetrameric Subunit Stoichiometry of Slc26 Proteins

Richard Hallworth[1], **Kelsey Stark**[2], **Lyandysha Zholudeva**[4], **Benjamin Currall**[3], and **Michael G. Nichols**[4]

[1]Department of Biomedical Sciences, Creighton University School of Medicine, Omaha, Nebraska 68178, USA

[2]Doane College, Crete, Nebraska 68333, USA

[3]Department of Obstetrics, Gynecology, and Reproductive Biology, Brigham and Women's Hospital, Boston, Massachusetts 02115, USA

[4]Department of Physics, Creighton University, Omaha, Nebraska 68178, USA

Abstract

The Slc26 family proteins, with one possible exception, transport anions across membranes in a wide variety of tissues in vertebrates, invertebrates, and plants. Mutations in human members of the family are a significant cause of disease. Slc26 family proteins are thought to be oligomers, but their stoichiometry of association is in dispute. A recent study, using sequential bleaching of single fluorophore-coupled molecules in membrane fragments, demonstrated that mammalian Slc26a5 (prestin) is a tetramer. In this report, the stoichiometry of two non-mammalian prestins and three human SLC26 proteins has been analyzed by the same method, including the evolutionarily-distant SLC26A11. The analysis showed that tetramerization is common and likely to be ubiquitous among Slc26 proteins, at least in vertebrates. The implication of the findings is that tetramerization is present for functional reasons.

Keywords

hair cell; outer hair cell; prestin; pendrin; Slc26

Introduction

The Slc26 family proteins are functionally important anion transport proteins. The family has ten known members. They exhibit diverse anion specificities and mechanisms, including single anion transport, paired exchange, and some members also act as ion channels to some substrates. The Slc26 family includes one member (Slc26a5), the protein product of which is prestin. Mammalian prestin may (Bai et al., 2009; Mistrik et al., 2012; Schanzler and Fahlke, 2012) or may not (Schaechinger and Oliver, 2007; Tang et al., 2012) transport anions, but is essential for hearing, as demonstrated by knock-out and knock-in mouse models (Dallos et al., 2008; Liberman et al., 2002).

Mutations of human SLC26 proteins are involved in several significant disease processes. Some mutations in SLC26A4, the protein product of which is pendrin, result in Pendred syndrome, which involves both a progressive hearing loss and goiter, while other mutations

Corresponding Author: Richard Hallworth Department of Biomedical Sciences Creighton University 2500 California Plaza Omaha, NE 68178 *Phone:* (402) 280-3057 *FAX:* (402) 280-2690 hallw@creighton.edu.

lead to the non-syndromic hearing loss DFNB4 (Kere, 2006). Mutations in SLC26A2 result in dystrophic dysplasia, while mutations in SLC26A3 result in congenital chloride diarrhea. Although they are limited to a few kindreds, mutations in SLC26A5 have been linked to sensorineural hearing loss (Liu et al., 2003; Teek et al., 2009; Toth et al., 2007).

All Slc26 proteins appear to be oligomers, but the stoichiometry of association has been in dispute. One study used blue native polyacrylaminde gel electrophoresis (BN-PAGE) to suggest that rat prestin, a zebrafish ortholog (*Danio rerio* Slc26a5), a human paralog (*Homo sapiens* SLC26A3), and a prokaryotic homolog (*Pseudomonas aeruginosa* SulP) all formed homo-dimers (Detro-Dassen et al., 2008). Another study suggested that, while the pendrin can form dimers, it more likely exists as a monomer (Porra et al., 2002). Analyses of prestin by Western blots and an electron density map have variously suggested dimeric or tetrameric configurations (Detro-Dassen et al., 2008; Mio et al., 2008; Zheng et al., 2006). A Western blot study also suggested that dimeric configurations were a common feature of Slc26 proteins (Detro-Dassen et al., 2008). However, the methods employed have limitations, including that the proteins are not in their native environment, the plasma membrane.

A recent study analyzed the sequential bleaching of single molecules of enhanced green fluorescent proteins (eGFPs) coupled to prestin in membrane fragments (Hallworth and Nichols, 2012). A plasmid expressing prestin-eGFP was transfected into the Human Embryonic Kidney (HEK) cell line. The presence of mature prestin protein in the plasma membrane was confirmed by electrophysiological methods and by optical correlation of the eGFP fluorescence with the binding of wheat germ agglutinin coupled to Alexa Fluor 568 (Currall et al., 2011b). Isolated membranes, attached to the glass bottom of a culture dish, were obtained by osmotic lysis. Single molecules of eGFP were detected using a high numerical aperture objective and a cooled electron-multiplying charge-coupled device camera. The preparations were sequentially imaged under continuous low-level excitation from a mercury source until all or most fluorophores were bleached to background level. The fluorescence of single-molecules over time was analyzed off-line using code written in MatLAB. Single molecule fluorescence was found to decrease in discrete approximately equal steps, which were taken to signify the bleaching of single eGFP molecules. By counting the number of steps required to bleach the single prestin-eGFP molecules to background fluorescence levels (with a correction for inherently dark fluorophores), the study determined that prestin in membranes adopts a tetrameric configuration. This method overcomes the limitations of previous methods because the protein is in its natural environment, the plasma membrane.

The existence of a common stoichiometry among Slc26 protein molecules would suggest the existence of common functional mechanisms. This study presents the analysis of the membrane stoichiometry of a comprehensive range of Slc26 proteins, using the same method of bleach step counting. Included in the measurement set were a mammalian prestin (gerbil prestin, gPres), and the orthologous chicken and zebrafish prestins (cPRES, zpres), which are not motor proteins and function as conventional anion transporters (Schaechinger and Oliver, 2007). The proteins analyzed also included three mammalian (human) paralogs: SLC26A4, SLC26A9, and SLC26A11, which is the most divergent of the family in our analysis.

Materials and Methods

1. Plasmids, Cells, and Transfection

A plasmid encoding gerbil prestin in frame with eGFP was a gift from Peter Dallos, Northwestern University. A plasmid encoding the gene for human ORAI1, coupled c-

terminal to eGFP, was a gift from Michael Cahalan, University of California-Irvine (Penna et al., 2008). Plasmids expressing cPRES and zPres cDNA were gifts from Dominic Oliver (Phillips University, Marburg) and were cloned in-frame with eGFP. Plasmids containing cDNA for the human SLC26A4, SLC26A9, and SLC26A11 genes were obtained from Open Biosystems (Thermo Scientific, Huntsville, AL). Plasmids containing the SLC26A4 and SLC26A9 genes in frames with eGFP were gifts from David He (Creighton University) and have been demonstrated to transport anions (D.Z.Z. He, personal communication). A plasmid encoding the gene for SLC26A11 in frame with eGFP was created by standard methods.

Cells (HEK 293) were cultured on glass-bottomed culture dishes (MatTek, Ashland, MA). Transfections of 60–80% confluent cells were performed using Lipofectamine 2000 (Invitrogen) following the manufacturer's instructions.

2. Osmotic Lysis Method

Dishes of cells were observed 12–24 hours after transfection. Cells were lysed using the method of Hallworth and Nichols (2012). Cells were exposed to a hypoosmotic buffer in the cold for 30 mins. The buffer consisted of 4 mM PIPES and 30 mM KCl (pH 7.8, 80 mOsm). Cells were then repeatedly subjected to a stream of buffer delivered via a blunted 28 gauge hypodermic needle.

3. Observation of eGFP Fluorescence

Sequences of fluorescence images were acquired using a DU-897E cooled back-thinned electron-multiplying charged-coupled device camera (Andor Technology, Belfast, Northern Ireland). Excitation and observation were performed using a mercury excitation source filtered by either a standard fluorescein filter set or a filter set specific for eGFP (Chroma Endow long pass, 41018, Chroma Technology, Bellows Falls, VT). A neutral density filter attenuated the excitation to retard bleaching. The camera electronics were cooled to −70°C.

Presumed membrane fragments containing fluorescence were observed at room temperature on the stage of an Olympus IX-70 inverted fluorescence microscope via a 100x magnification, 1.40 numerical aperture objective. Images were typically acquired for 1500 frames at 0.2 s per frame over a 128 by 128 or 256 by 256 pixel image (equivalent to 19.2 by 19.2 μm or 38.4 by 38.4 μm).

4. Analysis of Single-Molecule eGFP Fluorescence

The analysis of single molecule fluorescence is illustrated in Fig. 1. Regions of interest (ROIs) containing putative single molecule fluorescence were distinguished from random noise by following the ROI over sequences of images. Consecutive pairs of images in a stored sequence were averaged and the resulting images spatially filtered. Background subtraction was performed using an estimate of the background fluorescence of each image as a function of time, using a 9 pixel by 9 pixel ROI (1350 nm by 1350 nm) placed adjacent to but not overlapping potential single molecules. Analysis of image sequences was performed using a procedure developed in MatLAB (The MathWorks, Natick, MA). Images were smoothed using a 3 point low-pass spatial filter. A clipped ROI, overall dimensions 5 pixels by 5 pixels (750 nm by 750 nm), was selected to encompass putative single-molecule fluorescent points. The total fluorescence (in arbitrary units) of the point was calculated for each image in a sequence using the clipped ROI illustrated in Fig. 1A as a mask. The summed ROI fluorescence was then averaged, and the values were stored and plotted in temporal order as a record.

In all records, instantaneous or near-instantaneous step decrements in fluorescence were observed. These were presumed to be single eGFP molecule bleaching events. Records were analyzed only if the fluorescence reached background levels during the observations.

On the first analysis pass, step sizes were determined as the unsigned magnitudes of the step decrements in fluorescence in each record. Step sizes were determined by inspection using a custom procedure written in MATLAB (The MathWorks, Inc., Natick, MA). The sizes of all observed steps in an experiment were then pooled and plotted in histogram form. The distribution of step sizes was fitted to the sum of two Gaussian functions as follows:

$$y=\frac{A_1}{\sigma_s\sqrt{2\pi}}\exp\left(-\frac{(x-\mu_s)^2}{2\sigma_s^2}\right)+\frac{A_2}{2\sigma_s\sqrt{2\pi}}\exp\left(-\frac{(x-2\mu_s)^2}{8\sigma_s^2}\right) \quad (2)$$

where A_1 and A_2 are positive constants and μ_s and σ_s are the mean and the standard deviation. Fits were obtained using the Levenberg-Marquardt non-linear curve-fitting algorithm in Origin (OriginLab Corp., Northampton, MA). Experimental data were rejected if the correlation coefficients (R^2) were less than 0.9.

For each putative single molecule, the step count (the observed number of steps to bleach the ROI to background levels) was determined by inspection of the record, informed by the average step size μ as determined above. The fluorescence in most ROIs reached background fluorescence levels, as determined by sampling the fluorescence of ROIs adjacent to the point, within 1500 frames. All putative single molecule observations meeting the above criteria were included in the analysis.

The distribution of step counts was plotted in histogram form. As demonstrated in our previous paper (Hallworth and Nichols, 2012), and elsewhere (Ji et al., 2008; Madl et al., 2011; Ulbrich and Isacoff, 2007), not all eGFP molecules fluoresce. In the previous study, the fraction of functional eGFP molecules was about 65%, the remaining 35% being presumed to be dark. To correct for dark fluorophores, we analyzed the step count histogram using a binomial model, in which the fraction of fluorescing fluorophores was assigned the value p, the fraction of non-fluorescing fluorophores is q ($= 1- p$), and the integer sample size is n. The step count histogram was fit to a binomial sampling distribution as follows:

$$y=A\left(\frac{n!}{x!\,(n-x)!}\right)p^x q^{(n-x)} \quad (3)$$

where p and q are as defined above, A is a positive constant, and n is the integer sample size, which in these experiments corresponds to the stoichiometry of the molecule.

5. Determination of Stoichiometry

The step count histograms could often be fit to varying degrees by a range of p and n values. In these experiments, we assumed that p would be the same for each Slc26 protein, because it is presumably an intrinsic property of *eGFP* in our expression system. However, the mean of a binomial distribution, μ, is np. We therefore made three independent measures of μ from three experiments on gPres coupled to eGFP. We assumed tetrameric stoichiometry ($n = 4$), based on the findings of Hallworth and Nichols (2012) and then calculated p for each experiment. We then calculated our estimate of p, p_{est}, as the average of those three determinations. For subsequent experiments, we computed the average step count μ_c from the data, and estimated the stoichiometry n from μ_c/p_{est}.

6. Bioinformatics

The evolutionary history of the Slc26 family was inferred by using the Maximum Likelihood method based on the JTT matrix-based model (Jones, et al., 1992). Amino residue sequences were curated from either Ensembl (using predefined homology) or NCBI (using BLAST). The analysis involved 42 amino acid sequences. All positions containing gaps and missing data were eliminated. There were 299 positions in the final dataset. Multiple sequence alignment (MSA) and phylogeny analysis were performed using Mega5 (Tamura et al., 2011). The MUSCLE algorithm was applied for MSA and a maximum likelihood tree algorithm used to calculate phylogeny. Initial tree(s) for the heuristic search were obtained automatically as follows. When the number of common sites was < 100 or less than one fourth of the total number of sites, the maximum parsimony method was used; otherwise the BIONJ method with the MCL distance matrix was used.

Results

1) Evolutionary Relationships of Slc26 Proteins

To define a suitable selection of Slc26 sequences, we examined their evolutionary distance, as described in the Methods section. The results are shown in Fig. 2. As expected, cPRES and zpres Slc26a5 orthologs were closely related to mammalian prestin. Slc26a6 orthologs were closely related to the Slc26a5 orthologs and the two combined represented a major branch in Slc26 phylogeny. The next closest branches in the Slc26 family were found to be the Slc26a3 and Slc26a4 paralogs, followed by the Slc26a8 and Slc26a9 paralog. The most distant protein to prestin was the Slc26a11 paralogs. By this analysis, gPres, cPRES, and zpres were considered good representatives of both mammalian and non-mammalian orthologs. SLC26A4, SLC26A9, and SLC26A11 are representatives from major branches in the Slc26 family of proteins and their analysis would therefore provide a comprehensive survey of stoichiometry in Slc26 proteins.

2) Estimation of the Fraction of Fluorescing eGFP molecules, p_{est}

As described in the Methods section, we used measurements on gPres to establish an independent estimate of p for eGFP in our expression system (p_{est}), which was then used to determine the stoichiometry of the Slc26 orthologs and paralogs. A representative example of the three experiments used in the determination of p_{est} is shown in Fig. 3. We took gPres to be a tetramer, as had previously been established (Hallworth and Nichols, 2012). In the three experiments, we found the average step count μ_c to be 2.81, 2.64, and 2.80 (see Table 1). The computed value of p for each experiment was then 0.70, 0.66, and 0.70, the average of which (p_{est}) was 0.69 (± 0.1). This value corresponds closely to the value of p observed in (Hallworth and Nichols, 2012) for gPres, which was 0.67.

As a positive control, we performed three methodologically identical experiments with a plasmid expressing the dimeric protein Orai1, coupled to eGFP. A representative example of the three experiments is shown in Fig. 4A. Fig. 4A1 shows the distribution of step sizes, from which the average step size μ_s was determined, as shown in the figure, along with the standard deviation σ_s. We then determined the step count for each fluorescent point observed, using the average step size for that experiment μ_s as a guide where ambiguity existed. We then calculated the values of n for each experiment, using the average step counts μ_c divided by p_{est}. As shown in Table 2, the computed n was two (rounded to the nearest integer) in all three experiments. Thus we concluded that the step counting method and binomial analysis reliably determines the stoichiometry. The experimentally-observed distribution of step counts is shown in Fig. 4A2, along with the predicted distribution of step counts for the same number of observations N, assuming $n = 2$ and p_{est} is 0.67. The agreement is remarkable.

3) Sequential Bleaching Analysis of Prestin Proteins

We first examined stoichiometry in mammalian prestin and the non-mammalian prestins cPRES and zpres, using the single molecule sequential bleaching analysis described in the Methods section. Representative examples of the three experiments used in each determination are shown in Figs. 4B and 4C. We measured the average step size and average step count in experiments that were methodologically identical as that for gPres and ORAI1, and calculated the stoichiometry from the average step counts μ_c divided by p_{est}. As shown in Table 2, in both cases the calculated value of n, when rounded, was four, which we interpret as the number of subunits in each molecule.

4) Sequential Bleaching Analysis of Slc26 Family Proteins

We then tested the stoichiometry of the three SLC26 paralogs using the same experimental and analytical methods. Representative experiments on each are shown in Fig. 5. As shown in Table 2, in three experiments on each protein we found average step counts that, when divided by p_{est}, resulted in values of n (i.e., the stoichiometry of the molecules) consistent with tetramerization.

Discussion

Comparison of the Single Molecule Sequential Bleaching Approach with Previous Studies

Our findings imply that tetramerization is a consistent feature of vertebrate Slc26 proteins from widely divergent lineages. The implication is that tetramerization is universal in the family, at least in vertebrates.

The sequential bleaching method of determining subunit stoichiometry is not original to us and has been successfully applied to membrane proteins in several recent studies (Das et al., 2007; Durisic et al., 2012; Ji et al., 2008; Penna et al., 2008; Ulbrich and Isacoff, 2007). In some of these studies, the method was tested against membrane proteins of known stoichiometry and found to yield the correct result (Hallworth and Nichols, 2012; Ji et al., 2008; Ulbrich and Isacoff, 2007). The method does not rely on biochemical approaches that remove the proteins from their normal lipid environment. In contrast, gel-based methods to the study of stoichiometry of Slc26 proteins have given contradictory results. The BN-PAGE approach used in Detro-Dassen et al. (2008), which yielded dimeric configurations for three Slc26 proteins including prestin, is thought to at least reduce the effects of solubilization on membrane proteins. However, the same claim of non-denaturing properties was also made for the perfluoro-octonoate–PAGE western blot used by Zheng et al. (2006), and that study yielded tetramers of prestin from both yeast and TSA-201 expression systems. Further, the n-dodecyl β-D-mannoside purification of prestin from membranes yielded particles that had four-fold symmetry on examination by electron density mapping (Mio et al., 2008).

A possible resolution of the disparity in the results may be found in the study of by Zheng et al. (2006). This study found that that the tetrameric association of prestin was weak, in that it was broken down in lithium dodecyl sulfate, whereas the dimer association was resistant even to β-mercaptoethanol. The authors suggested in effect that .prestin is a dimer of dimers. It is therefore possible that the Detro-Dassen study saw only the stronger dimer interaction and missed the weaker “dimer of dimers interaction”, which was perhaps more likely to be preserved in our approach.

The single molecule sequential bleaching method has its limitations, and these are extensively discussed in {Hallworth, 2012 #11003}. The high levels of shot noise compared to the beaching step size effectively limits stoichiometry determination to single-digit

numbers. It is also certainly possible that smaller levels may exist undetected in the noise of our records. However, the Gaussian fits to the histograms of our step size results (which had correlation coefficients of greater than 0.9), strongly suggest that we are studying a uniform population of bleaching events, consistent with the bleaching of single eGFP molecules. Finally, the uncertainty of the determination of the value of p in our approach confers some uncertainty about the determination of n. However, the correct prediction of the stoichiometries of CNGA3 (in our previous study) and ORAI1 here reinforce confidence in our results.

Implications of Tetrameric Oligomerization

We suggest that, because tetramerization has been preserved in evolution, it is likely to be functionally important to Slc26 proteins. We further suggest that there may be oligomerization motifs common to members of the Slc26 family. Our suggestion is supported by a recent fluorescence (or Förster) resonance energy transfer study that found, not only homo-oligomerization between identical Slc26 subunits, but also hetero-oligomerization between subunits of divergent Slc26 proteins (Currall et al., 2011a).

We have not yet had the opportunity to examine the stoichiometry of an invertebrate Slc26 protein, such as *Drosophila* prestin. We note that tetrameric oligomerization may not extend beyond the animal kingdom. A recent study using small angle neutron scattering demonstrated that an Slc26 transporter from *Yersinia enterocolitica* purifies as a dimer (Compton et al., 2011).

Possible Oligomerization Motifs

A likely location for the oligomerization motifs is the carboxy terminal. In all Slc26 proteins so far studied, the carboxy terminal is large and intracellular (in mammalian prestin it comprises 247 of the overall 744 residues). In Slc26 proteins, the carboxy terminal includes a large domain with homology to the bacterial spoIIAA proteins, the Sulfate Transporter and Anti-Sigma factor (STAS) domain. Fragments encompassing 200 or more residues of the STAS domain have been shown to self-associate in solution (Pasqualetto et al., 2008). However, in Y. *enterocolitica* purified dimeric protein, the carboxy terminals face away from each other, thus their interaction motifs must lie elsewhere (Compton et al., 2011).

Cooperativity in the Slc26 Family

As suggested above, the ubiquity of tetramerization in the Slc26 family suggests it has a functional role. It is natural to ask if the subunits act cooperatively to effect ion transport. There is very little evidence for or against cooperativity in the Slc26 family. For the atypical Slc26 protein prestin, which is not primarily an anion transporter, contradictory evidence exists. One study found cooperative interactions between dual mutated copies of prestin (Detro-Dassen et al., 2008). However, another study, using an indirect measure of function, found no such evidence in the native protein (Wang et al., 2010). The resolution of this question must await a deeper understanding of the relationship between structure and function in the Slc26 family of proteins.

Acknowledgments

We thank Peter Dallos, David Z.-Z.He, Dominic Oliver and Michael Cahalan for plasmid constructs. We also thank Heather Jensen-Smith and our anonymous reviewers for helpful comments on the manuscript

Grants Supported by National Science Foundation-Nebraska EPSCoR EPS-0701892 to RH, State of Nebraska LB 692 to RH, and National Institutes of Health (NIH) GM085776 to MGN. Research was conducted in a facility constructed with support from Research Facilities Improvement Program C06 RR17417-01 from the National Center for Research Resources (NCRR) of the NIH.

References

BAI JP, SURGUCHEV A, MONTOYA S, ARONSON PS, SANTOS-SACCHI J, NAVARATNAM D. Prestin's anion transport and voltage-sensing capabilities are independent. Biophys J. 2009; 96:3179–3186. [PubMed: 19383462]

COMPTON EL, KARINOU E, NAISMITH JH, GABEL F, JAVELLE A. Low resolution structure of a bacterial SLC26 transporter reveals dimeric stoichiometry and mobile intracellular domains. J Biol Chem. 2011; 286:27058–27067. [PubMed: 21659513]

CURRALL, B.; JENSEN-SMITH, H.; HALLWORTH, R. Homo- and hetero-oligomerization in the Slc26a protein family. In: Shera, CA.; Olson, ES., editors. What Fire is in Mine Ears: Progress in Auditory Biomechanics. American Institute of Physics; Melville, NY: 2011a. p. 148-153.

CURRALL B, ROSSINO D, JENSEN-SMITH H, HALLWORTH R. The roles of conserved and nonconserved cysteinyl residues in the oligomerization and function of mammalian prestin. J Neurophysiol. 2011B; 106:2358–2367. [PubMed: 21813750]

DALLOS P, WU X, CHEATHAM MA, GAO J, ZHENG J, ANDERSON CT, JIA S, WANG X, CHENG WH, SENGUPTA S, et al. Prestin-based outer hair cell motility is necessary for mammalian cochlear amplification. Neuron. 2008; 58:333–339. [PubMed: 18466744]

DAS SK, DARSHI M, CHELEY S, WALLACE MI, BAYLEY H. Membrane protein stoichiometry determined from the step-wise photobleaching of dye-labelled subunits. Chembiochem. 2007; 8:994–999. [PubMed: 17503420]

DETRO-DASSEN S, SCHANZLER M, LAUKS H, MARTIN I, ZU BERSTENHORST SM, NOTHMANN D, TORRES-SALAZAR D, HIDALGO P, SCHMALZING G, FAHLKE C. Conserved dimeric subunit stoichiometry of SLC26 multifunctional anion exchangers. J Biol Chem. 2008; 283:4177–4188. [PubMed: 18073211]

DURISIC N, GODIN AG, WEVER CM, HEYES CD, LAKADAMYALI M, DENT JA. Stoichiometry of the human glycine receptor revealed by direct subunit counting. J Neurosci. 2012; 32:12915–12920. [PubMed: 22973015]

HALLWORTH R, NICHOLS MG. Prestin in HEK cells is an obligate tetramer. J Neurophysiol. 2012; 107:5–11. [PubMed: 21975444]

JI W, XU P, LI Z, LU J, LIU L, ZHAN Y, CHEN Y, HILLE B, XU T, CHEN L. Functional stoichiometry of the unitary calcium-release-activated calcium channel. Proc Natl Acad Sci U S A. 2008; 105:13668–13673. [PubMed: 18757751]

KERE, J. Epithelial Anion Transport in Health and Disease: the Role of the SLC26 Transporters Family (Wiley). 2006. Overview of the SLC26 family and Associated Diseases.

LIBERMAN MC, GAO J, HE DZ, WU X, JIA S, ZUO J. Prestin is required for electromotility of the outer hair cell and for the cochlear amplifier. Nature. 2002; 419:300–304. [PubMed: 12239568]

LIU XZ, OUYANG XM, XIA XJ, ZHENG J, PANDYA A, LI F, DU LL, WELCH KO, PETIT C, SMITH RJ, et al. Prestin, a cochlear motor protein, is defective in non-syndromic hearing loss. Hum Mol Genet. 2003; 12:1155–1162. [PubMed: 12719379]

MADL J, WEGHUBER J, FRITSCH R, DERLER I, FAHRNER M, FRISCHAUF I, LACKNER B, ROMANIN C, SCHUTZ GJ. Resting state Orai1 diffuses as homotetramer in the plasma membrane of live mammalian cells. J Biol Chem. 2011; 285:41135–41142. [PubMed: 20961852]

MIO K, KUBO Y, OGURA T, YAMAMOTO T, ARISAKA F, SATO C. The motor protein prestin is a bullet-shaped molecule with inner cavities. J Biol Chem. 2008; 283:1137–1145. [PubMed: 17998209]

MISTRIK P, DAUDET N, MORANDELL K, ASHMORE JF. Mammalian prestin is a weak Cl- / HCO3- electrogenic antiporter. J Physiol. 2012; 590:5597–5610. [PubMed: 22890707]

PASQUALETTO E, SEYDEL A, PELLINI A, BATTISTUTTA R. Expression, purification and characterisation of the C-terminal STAS domain of the SLC26 anion transporter prestin. Protein Expr Purif. 2008; 58:249–256. [PubMed: 18226918]

PENNA A, DEMURO A, YEROMIN AV, ZHANG SL, SAFRINA O, PARKER I, CAHALAN MD. The CRAC channel consists of a tetramer formed by Stim-induced dimerization of Orai dimers. Nature. 2008; 456:116–120. [PubMed: 18820677]

PORRA V, BERNIER-VALENTIN F, TROUTTET-MASSON S, BERGER-DUTRIEUX N, PEIX JL, PERRIN A, SELMI-RUBY S, ROUSSET B. Characterization and semiquantitative analyses of pendrin expressed in normal and tumoral human thyroid tissues. J *Clin Endocrinol Metab*. 2002; 87:1700–1707. [PubMed: 11932304]

SCHAECHINGER TJ, OLIVER D. Nonmammalian orthologs of prestin (SLC26A5) are electrogenic divalent/chloride anion exchangers. Proc Natl Acad Sci U S A. 2007; 104:7693–7698. [PubMed: 17442754]

SCHANZLER M, FAHLKE C. Anion transport by the cochlear motor protein prestin. J Physiol. 2012; 590:259–272. [PubMed: 22063625]

TAMURA K, PETERSON D, PETERSON N, STECHER G, NEI M, KUMAR S. MEGA5: molecular evolutionary genetics analysis using maximum likelihood, evolutionary distance, and maximum parsimony methods. Mol Biol Evol. 2011; 28:2731–2739. [PubMed: 21546353]

TANG J, PECKA JL, TAN X, BEISEL KW, HE DZ. Engineered pendrin protein, an anion transporter and molecular motor. J Biol Chem. 2012; 286:31014–31021. [PubMed: 21757707]

TEEK R, OITMAA E, KRUUSTUK K, ZORDANIA R, JOOST K, RAUKAS E, TONISSON N, GARDNER P, SCHRIJVER I, KULL M, et al. Splice variant IVS2-2A>G in the SLC26A5 (Prestin) gene in five Estonian families with hearing loss. Int J Pediatr Otorhinolaryngol. 2009; 73:103–107. [PubMed: 19027966]

TOTH T, DEAK L, FAZAKAS F, ZHENG J, MUSZBEK L, SZIKLAI I. A new mutation in the human pres gene and its effect on prestin function. Int J Mol Med. 2007; 20:545–550. [PubMed: 17786286]

ULBRICH MH, ISACOFF EY. Subunit counting in membrane-bound proteins. Nat Methods. 2007; 4:319–321. [PubMed: 17369835]

WANG X, YANG S, JIA S, HE DZ. Prestin forms oligomer with four mechanically independent subunits. Brain Res. 2010; 1333:28–35. [PubMed: 20347723]

ZHENG J, DU GG, ANDERSON CT, KELLER JP, OREM A, DALLOS P, CHEATHAM M. Analysis of the oligomeric structure of the motor protein prestin. J Biol Chem. 2006; 281:19916–19924. [PubMed: 16682411]

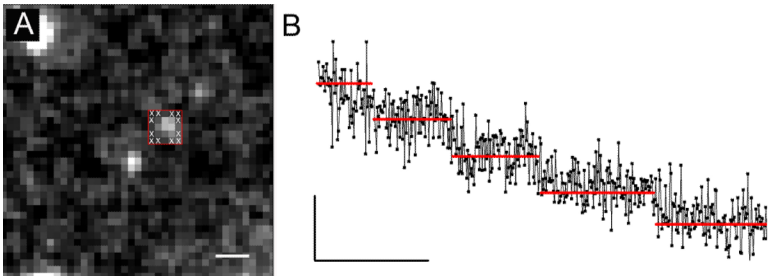

Figure 1.

A) Image of a single molecule showing the mask used for analysis. The scale bar represents 750 nm. B) Representative example of the time courses of fluorescence from experiments such as Figure 1A. The scale bars represent 50 s (time, horizontal) and 200 average counts (amplitude, vertical).

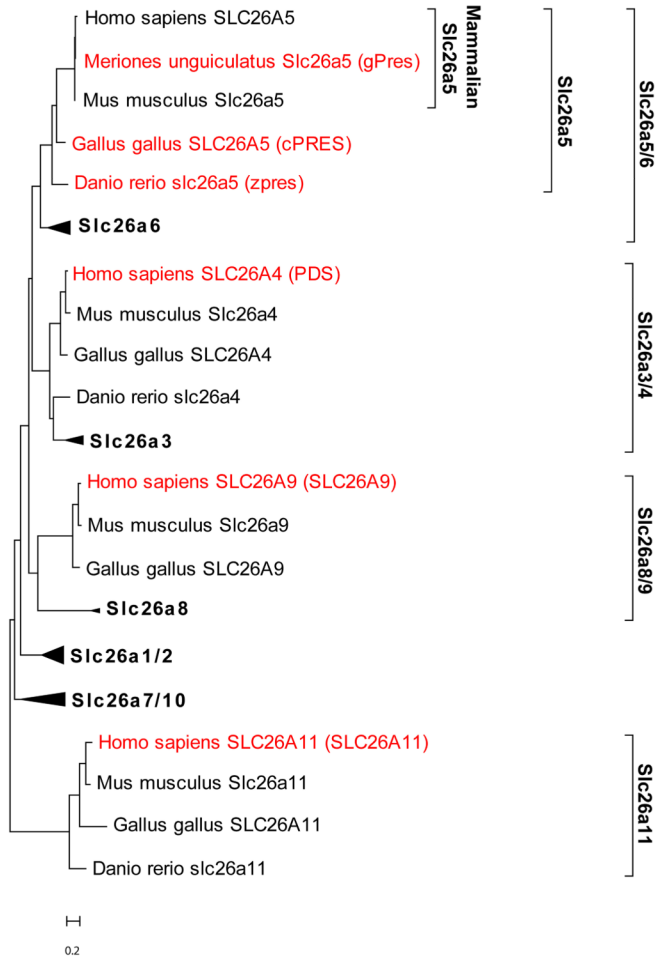

Figure 2.

Molecular phylogenetic analysis of Slc26 proteins by the Maximum Likelihood method. The tree with the highest log likelihood (−15058.5) is shown. The tree is drawn to scale. The scale bar represents the number of substitutions per residue.

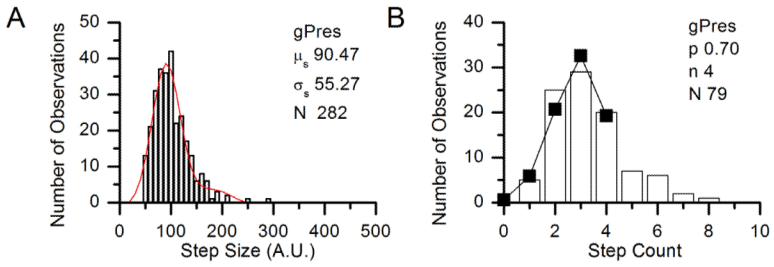

Figure 3.

Histograms of step size (A, in arbitrary units) and step counts (B) for a representative experiment in the determination of *p*. In A, the Gaussian fit parameters are given on the figure. The solid line and points in B shows the predicted distribution of step counts assuming $n = 4$.

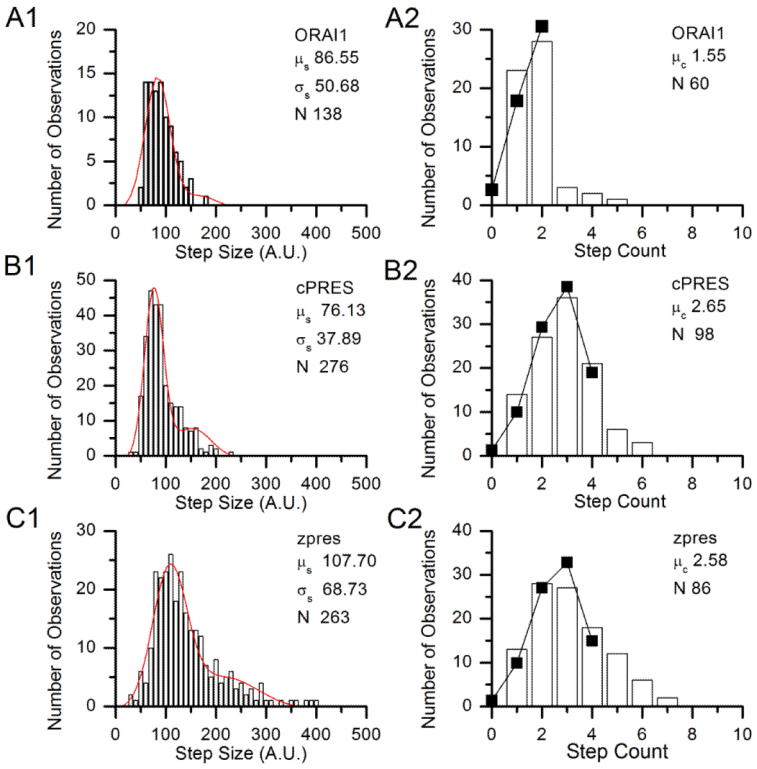

Figure 4.

Histograms of step size and step counts for single representative experiments in the determination of Slc26 stoichiometry. A) Histograms of step sizes (A1, in arbitrary units) and step counts (A2) from a single experiment on positive control ORAI1-eGFP. B) Histograms of step sizes (B1, in arbitrary units) and step counts (B2) from a single experiment on cPRES-eGFP. C) Histograms of step sizes (C1, in arbitrary units) and step counts (C2) from a single experiment on zpres-eGFP. The fit parameters for the step size distributions are given on the figures. In the step count histograms, the parameters show are the distribution mean μ_c and the number of points analyzed *N*. The solid lines and points show the predicted distribution of step counts assuming $p = pest = 0.69$ and n is the calculated integer value given in Table 2.

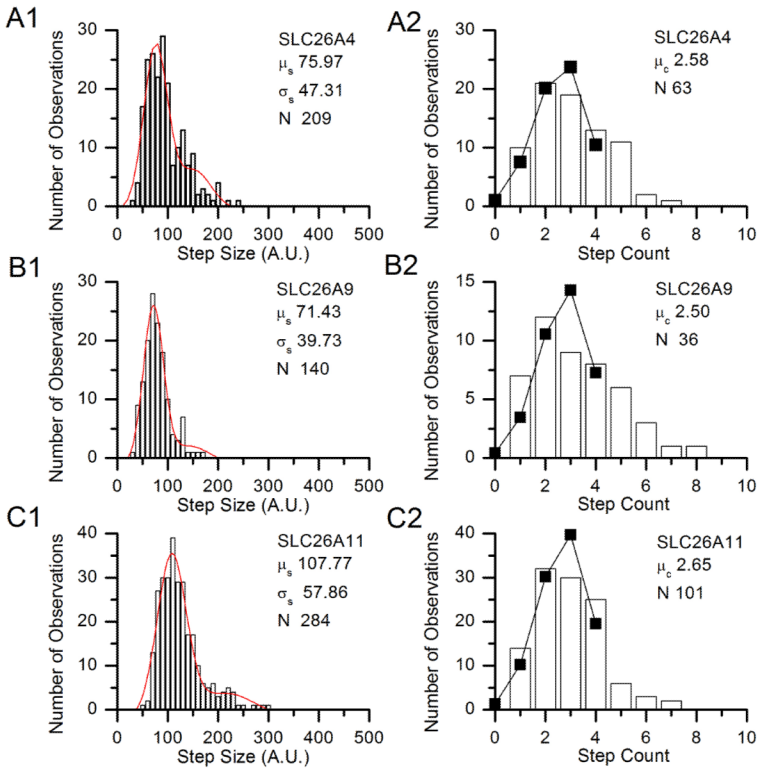

Figure 5.

Histograms of step size and step counts for single representative experiments on SLC26 paralogs. A) Histograms of step sizes (A1, in arbitrary units) and step counts (A2) from a single experiment on SLC26A4-eGFP. B) Histograms of step sizes (B1, in arbitrary units) and step counts (B2) from a single experiment on SLC26A9-eGFP eGFP. C) Histograms of step sizes (C1, in arbitrary units) and step counts (C2) from a single experiment on SLC26A11-eGFP eGFP. The fit parameters for the step size distributions are given on the figures. In the step count histograms, the parameters show are the distribution mean $\mu_{>c}$ and the number of points analyzed *N*. The solid lines and points show the predicted distribution of step counts assuming $p = pest = 0.69$ and *n* is the calculated integer value given in Table 2.

Table 1

Determination of p_{est}.

Step Count			
Number of molecules	***n***	**μ_c**	***p***
79	4	2.81	0.70
75	4	2.64	0.66
59	4	2.80	0.70
Mean (p_{est})			**0.69**
S.E.M.			**0.01**

Table 2

Determination of Slc26 Protein Stoichiometry.

Protein	Step Size		Step Count			Integer n (stoichiometry)
	μ_s	σ_s	Number of molecules	μ_c	Calculated n (= μ_c /p_{est})	
$ORAI_1$	65.28	31.48	50	1.42	2.07	*2*
	86.55	50.68	60	1.58	2.31	*2*
	83.45	49.67	51	1.55	2.26	*2*
cPRES	76.13	37.69	98	2.65	3.87	*4*
	110.06	75.52	242	2.63	3.83	*4*
	115.42	72.92	104	3.06	4.46	*4*
zpres	107.7	68.73	86	2.58	3.76	*4*
	111.05	64.41	52	2.85	4.15	*4*
	80.24	56.1	127	2.53	3.68	*4*
$SLC26A_4$	75.97	47.31	63	2.56	3.73	*4*
	84.92	46.2	57	2.42	3.53	*4*
	86.1	45.65	41	2.59	3.77	*4*
$SLC26A_9$	77.04	35.02	33	2.67	3.89	*4*
	71.43	39.73	36	2.50	3.64	*4*
	94.65	52.82	44	2.89	4.15	*4*
$SLC26A_{11}$	107.77	57.86	101	2.65	3.87	*4*
	105.12	59.83	89	2.53	3.69	*4*
	98.49	63.91	50	2.44	3.56	*4*